RSC Advances

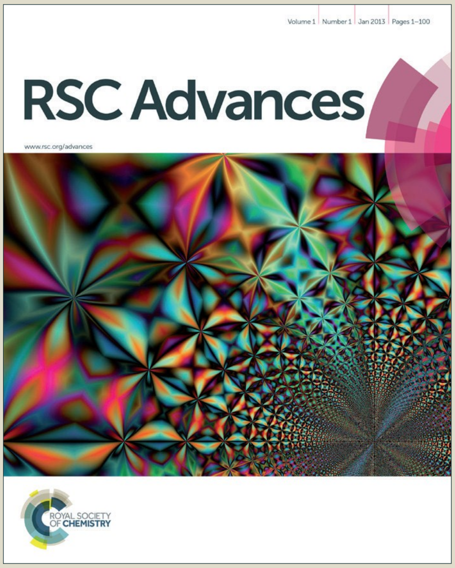

ROYAL SOCIETY
OF CHEMISTRY

www.rsc.org/advances

One-pot Synthesis of aminated multi-walled carbon nanotube using thiol-ene Click Chemistry for improvement of epoxy nanocomposites properties

Omid Zabihi[1], Mojtaba Ahmadi[2], Mostafa Akhlaghi bagherjeri[3], Minoo Naebe[1, *]

[1] Deakin University, Geelong, Australia, Carbon Nexus, Institute for Frontier Materials
[2]Department of Chemical Engineering, Isfahan University of Technology, Isfahan, 84156/83111, Iran
[3]Department of Chemistry, Ferdowsi University of Mashhad, Mashhad, Iran

Abstract:

A non-oxidative method based on thiol-ene Click Chemistry for functionalization of multi-walled carbon nanotube (CNT) was performed in order to improve the interfacial interactions between epoxy matrix and CNT. In this way, the CNT was aminated using 2-aminoethanethiol hydrochloride radicals thermally produced by a peroxide radical initiator. The aminated CNT ($CNT-NH_2$) was characterized by FTIR, TGA, and solubility evaluations, confirming that thiol radicals are successfully grafted onto the CNT surface with a proper yield. Various percentages of pure CNT (p-CNT) and $CNT-NH_2$ were then incorporated into epoxy matrix to evaluate the effect of the functionalization of CNT on thermal, mechanical, and morphological properties. The nanocomposites were characterized by DMA, tensile testing, and TGA. Results showed that glass transition temperature, tensile properties and thermal stability of epoxy nanocomposites containing $CNT-NH_2$ improves significantly compared to those containing unmodified CNT. These results prove the role of amino-functionalization in improving the interfacial adhesion between epoxy and CNT, which was further confirmed by morphological observations of fracture surfaces of the nanocomposites.

Keywords: Multi-walled Carbon Nanotubes; Click Chemistry; Interfacial Interactions, Epoxy nanocomposites

---

*Corresponding author: Tel: +613 5227 1410

E-mail: Minoo.Naebe@deakin.edu.au

1. Introduction

Since the discovery of carbon nanotubes in 1991 by Iijima (1), many studies have been focused on the properties and applications of these materials. Nowadays, a variety of nanotube types is available e.g. single wall nanotubes, double-wall nanotubes, and multi-wall nanotubes (2). CNTs which composed of cylindrical graphene sheet of sp^2-bonded carbon atoms possess outstanding mechanical, thermal, and electrical properties (3-6). High strength (~100 times stronger than steel) and modulus (about 1 TPa), high thermal conductivity (about twice as high as diamond), excellent electrical capacity (1000 times higher than copper), and thermal stability (2800°C in vacuum) in combination with low density and high aspect ratio, make CNTs one of the most promising candidates to reinforce polymer nanocomposites (7, 8). Moreover, compared to conventional fibers used in reinforcing of polymer-based microstructures, CNTs own much greater stress transfer efficiency attributed to its crack bridging effect (9, 10).

Among different polymer matrices for fabrication of CNTs reinforced nanocomposites, epoxy resins are widely used due to their properties arising from its highly cross-linked structure (11-16). The main drawback of epoxy resin for structural applications such as aerospace and automotive is its inherent brittleness (17), poor thermal properties (18, 19) and low resistance to crack initiation and propagation (20).

It has been proposed that the incorporation of CNTs in epoxy resin can improve mechanical and thermal properties of epoxy composites. However, ideal homogeneous CNTs reinforced epoxy and good interfacial interactions between the nanotubes and the epoxy matrix are extremely difficult to achieve due to large surface areas and strong van der Waals forces of attraction existed in CNTs (21-24). Furthermore, the carbon atoms on CNT walls are chemically stable due to the aromatic nature of the bond. Consequently, the reinforcing CNTs are inert and can interact with the surrounding matrix mostly via van der Waals interactions, unable to provide sufficient load-transfer across CNT/matrix interfacial region (25, 26). Therefore, selecting proper techniques for homogenous dispersion of CNTs in epoxy matrix and improvement of interaction between CNTs and epoxy resin is still a challenge in fabrication of CNTs reinforced polymer composites.

Various mechanical dispersion techniques, such as ultrasonication, calendering process, ball milling, stir and extrusion, are proposed to separate individual CNTs from CNT agglomerates and clusters. However, there are several concerns in using these techniques for dispersion of

CNT. For example, CNTs can be easily and seriously damaged as most of these approaches are too aggressive and/or too long, resulting in deteriorating of nanocomposites properties. In addition to mechanical techniques, there are two main chemical methods to improve CNT dispersion and ultimately interfacial interaction of nanotubes and matrix. These methods are physical functionalization (i.e. noncovalent attachment of molecules) and chemical functionalization (i.e. covalent attachment of functional groups) (27, 28). The major drawback of noncovalent attachment is that the interactions between the wrapping molecule and the sidewall of CNTs could be weak (e.g., hydrogen bonding, π-π stacking, electrostatic forces, van der Waals forces and hydrophobic interactions) which can result in low load transfer in nanocomposites. On the other hand, the covalent attachment of functional groups onto the surface of nanotube, via a change of hybridization from sp^2 to sp^3 and a simultaneous loss of π-conjugation system on graphene layer, can improve the efficiency of load transfer (29-32).

Recently, different functional groups, such as fluorine, carboxylic, hydroxyl, nitro, and amine groups, have been attached to tube ends or sidewalls of CNTs through chemical modification (33-35). As a result, a covalent bond between attached functional groups and the epoxy resin is formed and the interfacial interaction will be improved, promoting thermal and mechanical properties of CNT/epoxy nanocomposites. Among these functional groups, aminosilane functionalized CNTs has been widely studied due to being highly reactive as well as wealth of chemistry; and thus can be directly introduced into epoxy resin (36-43). According to Gonzalez-Dominguez et al. (44), incorporation of CNTs in which the sidewalls are functionalized with terminal primary amines, into trifunctional high-performance epoxy could improve the covalent anchoring between filler and matrix. On the contrary, it has been indicated that the un-functionalized CNTs or those aminated on tips and edges do not present any evidence of covalent bonds anchoring to the matrix. Ma et al. (45) declared that grafting 3-glycidoxypropyltrimethoxysilane molecules onto the CNT surface improved simultaneously the dispersion of CNTs and interactions between nanofillers and epoxy resin, leading to enhancement of mechanical and thermal properties as well as fracture resistance of nanocomposites compared to those containing untreated CNTs. Kathi et al. (46) modified CNTs via oxidation and silanization processes using acid mixture and 3-aminopropyltriethoxysilane, respectively. They showed that both silane-modified CNTs and oxidized CNTs could improve thermal and mechanical properties which is attributed to the good dispersibility and strong interfacial bonding between modified CNTs and the epoxy matrix. In addition, it was shown that the mechanical properties declined as the CNTs content exceeded 0.2 wt.%. This was due to agglomeration of CNTs resulting in non-uniform dispersion, stress concentration sites and voids. According to Cui et al. (47), addition of amino-functionalized CNTs improved tensile strength and nanofiller-matrix interfacial bonding as a result of uniform dispersion of CNTs in matrix. Shen et al. (48) showed that functionalization of CNTs with different amino groups could result in homogeneous dispersion of modified CNTs in epoxy, improvement of the thermal and mechanical properties of the composites which arise from strong interfacial CNTs-epoxy bonding as well as higher wettability.

Most approaches to functionalize CNTs with reactive functional groups are limited and hindered by side effects of oxidation process. Therefore, functionalization of CNTs via acid treatments and oxidizing agents, can significantly decrease CNTs aspect ratios and destroy their structures (42). Recently, direct functionalization of CNTs has been conducted via 1,3-dipolar cycloaddition, diazotization and thiol-ene click chemistry approaches, in which there is no need to introduce carboxylic acid and hydroxyl groups via oxidation process (49, 50). Among these direct chemical functionalization methods, thiol-ene click chemistry has been effectively applied in materials synthesis and modification due to its simplicity and high efficiency of reaction under mild conditions with a vast range of chemical species (51-54). In this study, for the first time, thiol-ene click chemistry approach has been applied to modify CNTs surface using 2-aminoethanethiol hydrochloride radicals to be used as an engineered filler for preparation of high-performance polymer nanocomposites. The role of this chemical modification in change of interfacial interactions between CNTs and epoxy resin has been comprehensively investigated by studying the mechanical and thermal properties of epoxy based nanocomposites.

2. Experimental

2.1. Materials

An epoxy resin of DER 332 having equivalent weight of 175 g/eq under trademark of The Dow Chemical Company and hardener of Dytek® EP diamine was used as thermosetting epoxy polymer system (Sigma-Aldrich). Multiwalled carbon nanotube supplied by Jiang Youg Trade Co. (China) with 30-50 μm length and 5-25 nm diameter was used in this study. Dicumyl peroxide (98%, Merck), 2-aminoethanethiol hydrochloride (AETH, Sigma, >97%), and sodium hydroxide (≥99%, Merck) were used as received. All the solvents used in this work were of ACS reagent.

2.2. CNT-NH_2 synthesis

A mixture of p-CNT (300 mg) and DMF (250 ml) was firstly sonicated for 1 h. In a two-necked round bottom flask dispersed CNT/DMF was blended with 2-aminoethanethiol hydrochloride (11.35 ml, 0.1 mol) and dicumyl peroxide (13.51 g, 0.05 mol) and stirred at 120 ^{o}C for further 48 h under reflux condition and continuous nitrogen atmosphere. The mixture was cooled to ambient temperature and then 50 ml NaOH solution (1.5 N) was added in and stirred again for 1 h. The final mixture was diluted by 200 mL of deionized water, and the resulting mixture (CNT-NH_2) was filtered under vacuum and washed several times with abandon deionized water and acetone to remove any un-reacted chemicals.

2.3. Epoxy nanocomposites preparation

To prepare the epoxy nanocomposites, various amounts of the p-CNT and CNT-NH_2 (0, 0.1%, 0.2%, and 0.5%) were mixed with epoxy resin and stirred using a magnet bar at 60 ^{o}C for 1 h, followed by 2 h sonication in an ultrasonic bath. Then a stoichiometric amount of curing agent was added to the CNT/epoxy compositions. The mixtures were mechanically mixed again for 5 min and then poured into cure container. The curing reaction conducted according to the followings which contains two stages: 1) at 80 °C for 2 h in a vacuum oven, and 2) postcuring of samples at 100 °C for 30 min.

2.4. Measurements

FT-IR spectrum was recorded with a KBr pellet containing samples on a Shimadzu IR prestige-21 FTIR spectrophotometer. TGA experiments were carried out using a Thermogravimetry Analyzer (TGA-50, Shimadzu, Japan). Thermogravimetry experiments were conducted in nitrogen atmosphere at a heating rate of 10 ^{o}C/min from room temperature to 750 ^{o}C. Dynamic mechanical properties of the produced materials were measured using a DMA-TRITON. The samples were polished to ~30mm×10mm×1 mm before being mounted on a single cantilever clamp. The DMTA tests experimental conditions were: temperature range, 25–250 ^{o}C; frequency of 1 Hz; and heating rate 3 ^{o}C/min. Tensile properties of samples are determined on samples with dimensions of 25 mm×5 mm×1 mm using an Instron Universal Testing Machine. Five tests were conducted on each sample according to ASTM D638 and a cross-head speed of 1 mm/min was employed. SEM micrographs on the fracture surface of the nanocomposite films were obtained with a Philips field emission gun SEM (model: XL30, Netherlands) operated at 25 kV.

3. Result and discussion

3.1. CNT-NH_2 Characterizations

Fig. 1 shows the functionalization strategy of p-CNT to obtain the amine-rich CNT surface. According to the suggested mechanism, the free radicals are firstly produced from thermal decomposition of dicumyl peroxide, which are quite unstable. These radicals strongly tend to have electron valence by acquisition of a hydrogen radical from the thiol group of 2-aminoethanethiol hydrochloride, which lead to generating the corresponding thiol radicals. These thiol radicals are strong enough to break C=C bonds of CNT skeleton and consequently graft onto the surface (51).

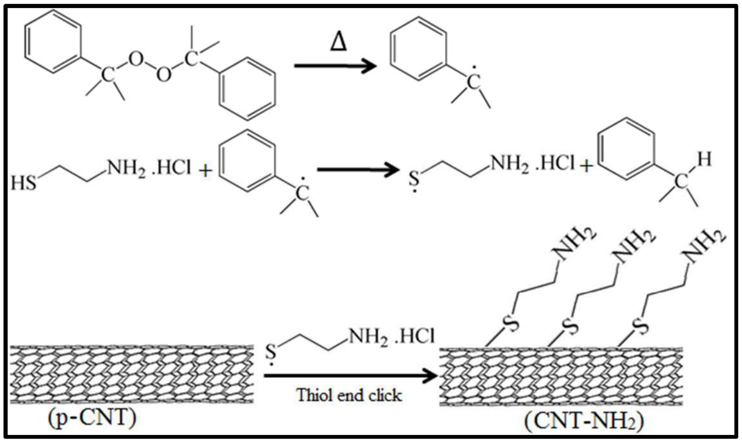

Fig. 1. Chemical synthesis route of CNT-NH_2 via thiol-end click chemistry.

In order to confirm the functionalization of p-CNT through thiol radicals, FTIR analysis were carried out on the p-CNT and CNT-NH_2, and their results are presented in Fig. 2a. For the p-CNT, the bonds of 3420 and 1100 cm^{-1} are attributed to the hydroxyl groups on the surface due to ambient atmospheric moisture. In addition, the p-CNT shows some weak absorption peaks between 2980-2840 cm^{-1} which is related to the –CH stretching absorption band. The –CH stretching bond as well as bond at 1625 cm^{-1} assigned to the carbonyl stretching of quinone groups indicate the presence of defects in CNT structure which is likely to be formed during its manufacturing. The FT-IR spectra of CNT-NH_2 presents a C–N stretching band at around 1050 cm^{-1}, indicating that amine groups were introduced on the p-CNT surface. Furthermore, the N–H stretching and the N–H deformation bonds of the primary amine groups, which appear at 3400 cm^{-1} and 1645 cm^{-1}, respectively, confirm successful reaction between 2-aminoethanethiol and p-CNT. The weak absorption of S-C bonds can be also observed at below 720 cm^{-1} region. TGA analysis was used to estimate the grafting yield of thiol radicals onto the surface. Fig. 2b shows typical weight loss of $CNT-NH_2$ at a wide temperature range, in which 5% and 12% weight loss occurs in 300 ^oC and 700 ^oC, respectively, in comparison to p-CNT. The $CNT-NH_2$ shows a lower weight loss compared to those functionalized via oxidation and silanization of CNT (43), which is because of the non-oxidative nature of this chemical functionalization. Furthermore, the weight loss of $CNT-NH_2$ between 100 ^oC and 700 ^oC is about 18%, which is slightly higher than that of other non-oxidative functionalization methods reported in the literature (44). Fig. 2c and 2d present morphologies of p-CNT and $CNT-NH_2$, respectively. As it can be seen, p-CNT shows a curly and intertwined morphology. Also, the diameter of the p-CNT is fairly uniform and no obvious block is observed. After functionalization reactions, it can be observed that the diameter of the $CNT-NH_2$ remains partly intact, which confirms that the performed functionalization is non-destructive. Furthermore, $CNT-NH_2$ severely intertwines with each other, resulting in a bigger CNT block forming.

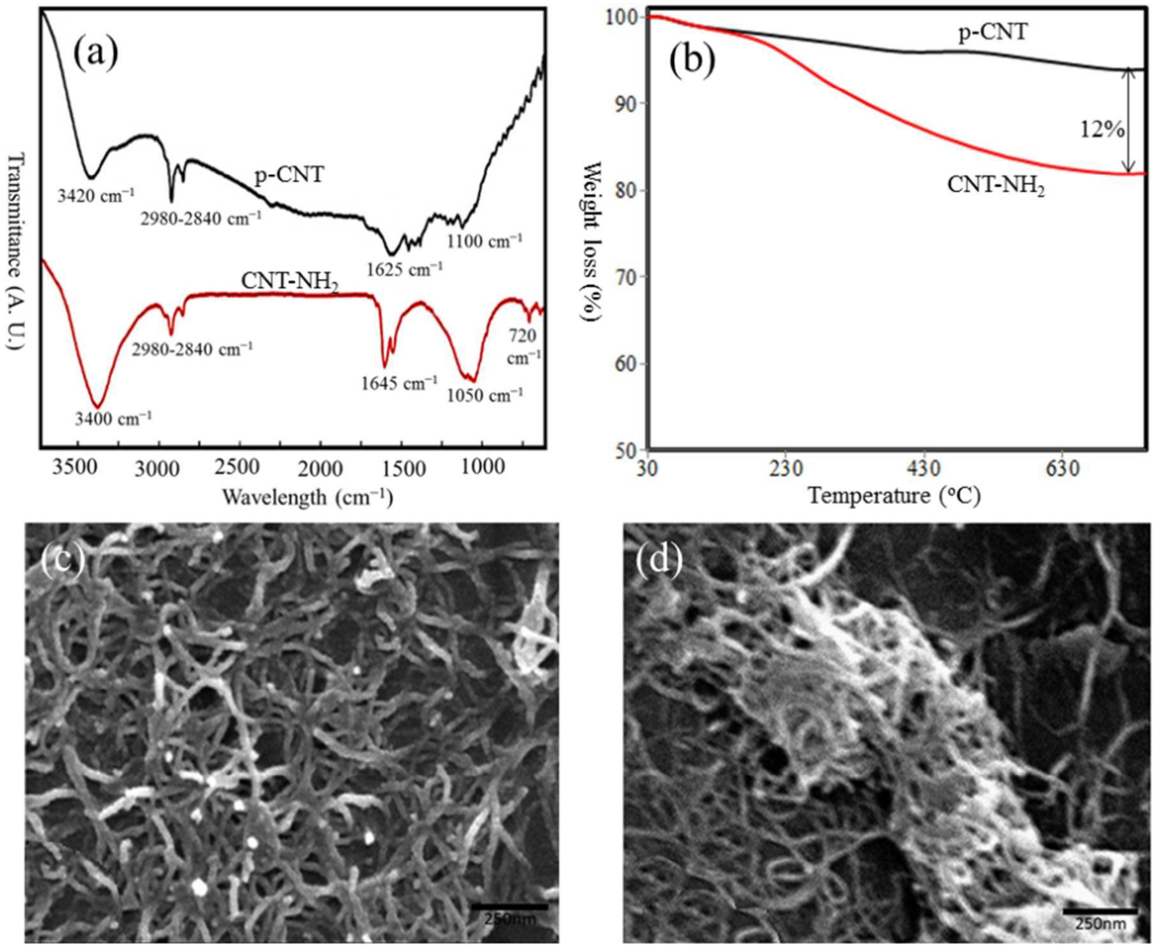

Fig. 2. (Top) FTIR spectrums (a) and TGA analysis (b) of p-CNT and $CNT-NH_2$; and (bottom) SEM images of p-CNT (c) and $CNT-NH_2$ (d).

The dispersion stability of CNTs in acetone as a polar aprotic solvent and ethanol as a polar protic solvent at two different time lengths (1 and 18 h) are shown in Fig. 3. The p-CNT and $CNT-NH_2$ were dispersed in the solvents by an ultrasonic bath and then their stabilities were photographed. As expected, the dispersibility of p-CNT in acetone is poor and it is gradually deposited after 1 h and is totally precipitated after 18 h. After functionalization of p-CNT, its dispersion behavior changed in both solvents. As can be seen in Fig. 3 c and d, $CNT-NH_2$ shows stable dispersions in acetone after 1 and 18 h, which is due to organic molecules grafted onto the surface, increasing the organophilicity of CNT. Although the organic molecules grafted onto the surface have the amine groups capable of hydrogen-bonding with aprotic solvent (e. g. ethanol), the $CNT-NH_2$ dispersibility in ethanol is not as stable as is in acetone and very gradually was precipitated after 18 h (Fig. 3e and 3d).

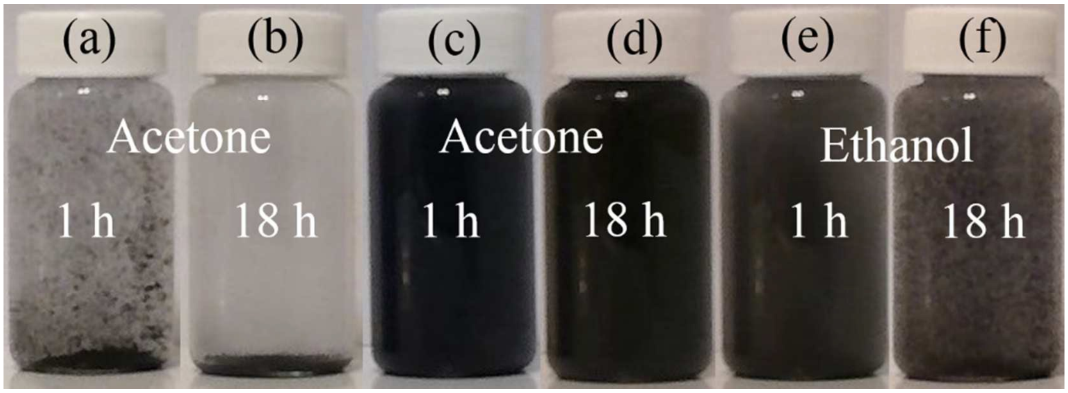

Fig. 3. Dispersibility profiles of p-CNT (a and b) and CNT-NH_2 (c, d, e, and f) in different time lengths and solvents.

3.2. DMTA Analysis of Epoxy Nanocomposites

As the amine groups can covalently react with epoxide groups of epoxy resin, effect of amine groups of CNT-NH_2 on the glass transition temperature (T_g) of the epoxy nanocomposites were examined by DMTA analysis. The measured T_g values of p-CNT/epoxy and CNT-NH_2/epoxy nanocomposites containing various CNT loadings are presented in Table 1. The CNT-NH_2/epoxy nanocomposites generally show higher T_g compared to p-CNT/epoxy nanocomposites. For both p-CNT and CNT-NH_2 epoxy nanocomposites, the T_g increases initially with CNT loading. Compared to pure epoxy, the p-CNT/epoxy and CNT-NH_2/epoxy nanocomposites show an increase of 1.4 ^{o}C and 6.5 ^{o}C, respectively, when the CNT loading is 0.1%. This improvement in T_g is attributed to the difference in the extent of crosslinking reactions of epoxy matrix. Given the same amount of CNT loading, the amine groups on CNT-NH_2 surface can covalently react with epoxy monomers and establish a higher degree of crosslinks in the epoxy matrix and consequently result in higher T_g. Regardless of CNT chemical functionalization, T_g increases with increasing the CNT loading up to 0.2%, as shown in Table 1. However, increase of T_g for epoxy systems containing CNT-NH_2 is higher than that of the p-CNT. We found that T_g values begin to decrease when the CNT loadings exceed 0.2 %, which is in agreement with other reports (46). This decrease in T_g could be due to an increase in agglomeration states at higher loadings, which hinder forming of a highly cross-linked matrix resulting in a decrease in degree of crosslinking in the nanocomposites. For better comparison, the crosslink density of the epoxy systems can be estimated using the following equation (55-58):

$$v_e = \frac{E_r}{3RT_r} \tag{1}$$

where v_e is the estimation of crosslink density, E_r is the rubber modulus which can be regarded as T_g+30, R is the universal gas constant, and T_r is T_g+30. The results of calculations are shown in Table 1, which demonstrate a direct relation between rubber modulus and T_g, which consequently affect the crosslink density of epoxy nanocomposites.

Table 1. Results of DMTA analyses for various epoxy nanocomposites.

	T_g (°C)		**E_r (GPa)**		**v_e (mmol/m^3)**	
CNT%	***p-CNT***	***CNT-NH$_2$***	***p-CNT***	***CNT-NH$_2$***	***p-CNT***	***CNT-NH$_2$***
0	81.3	81.3	0.42	0.42	43.7	43.7
0.1	82.7	87.8	0.56	0.71	58.2	72.8
0.2	84.4	91.5	0.57	0.75	58.9	76.2
0.5	84.1	89.3	0.49	0.74	50.7	75.6

3.3. Mechanical Properties of Epoxy Nanocomposites

The results of tensile strength and tensile modulus of the various epoxy nanocomposites are presented in Fig. 4. As is shown, the epoxy nanocomposites containing CNT-NH$_2$ show higher tensile strength and tensile modulus in comparison to those incorporated with p-CNT and pure epoxy itself. This indicates the strong interactions in interface of CNT-NH$_2$ with epoxy matrix. Tensile strength of epoxy nanocomposite slightly improves with addition of 0.1% CNT-NH$_2$, whereas 1% p-CNT inclusion result in decrease in tensile strength compared to pure epoxy. It is also observed that up to 0.2% loading, CNT-NH$_2$/epoxy systems show a better tensile strength in comparison to the p-CNT/epoxy systems. At 0.2% loading, the tensile strength at break of CNT-NH$_2$/epoxy nanocomposite increases from 42 MPa to 49 MPa, which is about 16% higher than that of pure epoxy, and a 7% increase as compared to the corresponding epoxy/p-CNT nanocomposite. It is also found that when the CNT loadings increase up to 0.5%, the tensile strength decreases in both CNT types. This decrease in high CNT loadings can be due to the increase of agglomeration in CNT bundles. Because of the high aspect ratio and high surface energy, CNT tend to aggregate and entangle together. Furthermore, the increasing viscosity with increasing the CNT loadings makes homogenous dispersion of CNT into epoxy matrix challenging. The tensile modulus of p-CNT/epoxy and CNT-NH$_2$/epoxy nanocomposites increase continuously even up to 0.5% CNT loading. At 0.5% loading, the tensile modulus improves by 55% and 31% for CNT-NH$_2$/epoxy and p-CNT/epoxy nanocomposite, respectively. The improved tensile modulus is attributed to the increased stiffness of the matrix, resulting from the reinforcement effect of CNT.

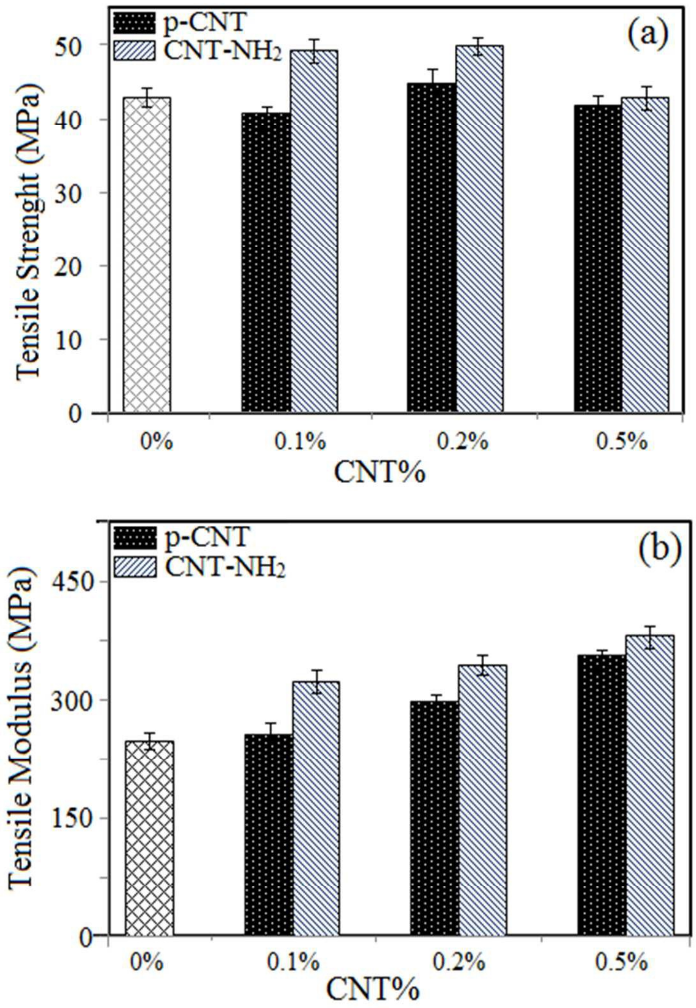

Fig. 4. Tensile strength (a) and tensile modulus (b) of epoxy nanocomposites containing various %loadings of CNTs.

3.4. Morphology of Epoxy Nanocomposites

SEM observations on the fracture surface of the pure epoxy and its nanocomposites are shown in Fig. 5. The surface of pure epoxy shows a river-like pattern (see Fig. 5 a), usually known as the feature of brittle fracture behaviour. The fracture surface between the lines of river is fairly smooth. The surface of epoxy nanocomposites exhibits a substantial increase in the surface roughness, which denotes the CNT reinforced matrix. The surface of epoxy nanocomposites containing 0.2% p-CNT is shown in Fig. 5b, observing that most of the p-CNT are aggregated due to their poor dispersion in the epoxy matrix. The magnified SEM image reveals that p-CNT are curled, entangled, and pulled out, confirming poor dispersion and weak interfacial bonding between p-CNT and epoxy matrix. Fig. 5c presents the fractured surface of 0.2 w% CNT-

NH_2/epoxy, which demonstrates that the amine groups on the surface has promoted the homogeneous dispersion of CNT-NH_2 in the epoxy resin; and the surface seems quite smooth throughout the cross-section. In addition, it can be also seen that the CNT-NH_2 are tightly embedded into the epoxy matrix, and as indicated by the arrows in Fig. 5c, some broken bundles of CNT-NH_2 can be easily observed, which shows improved interfacial bonding between CNT-NH_2 and epoxy. Nevertheless, at 0.5% CNT-NH_2 loading, the dispersion of CNT-NH_2 in the epoxy obviously decreased (see Fig. 5d). As it is pointed by arrows, many aggregated CNT-NH_2 regions can be observed throughout the surface. As shown in the magnified Fig. 5d, less uniformly dispersed and more highly entangled CNT-NH_2 are observed in the CNT-NH_2/epoxy nanocomposites with high CNT-NH_2 loading, which could explain decrease in the T_g and tensile strength of the CNT-NH_2/epoxy nanocomposites observed earlier at higher loading.

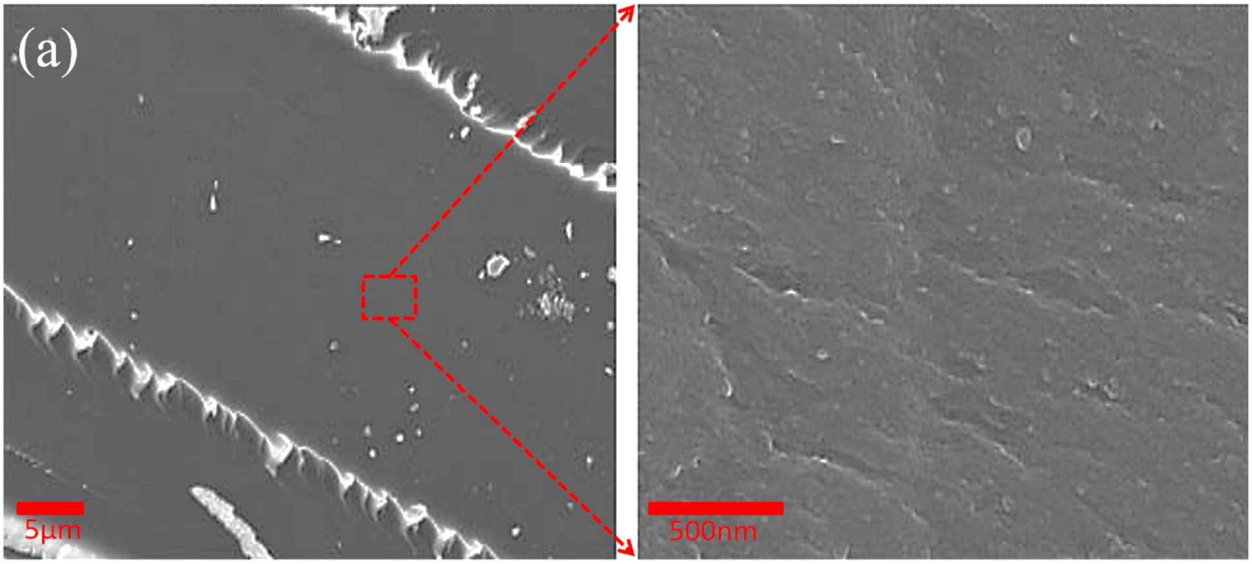

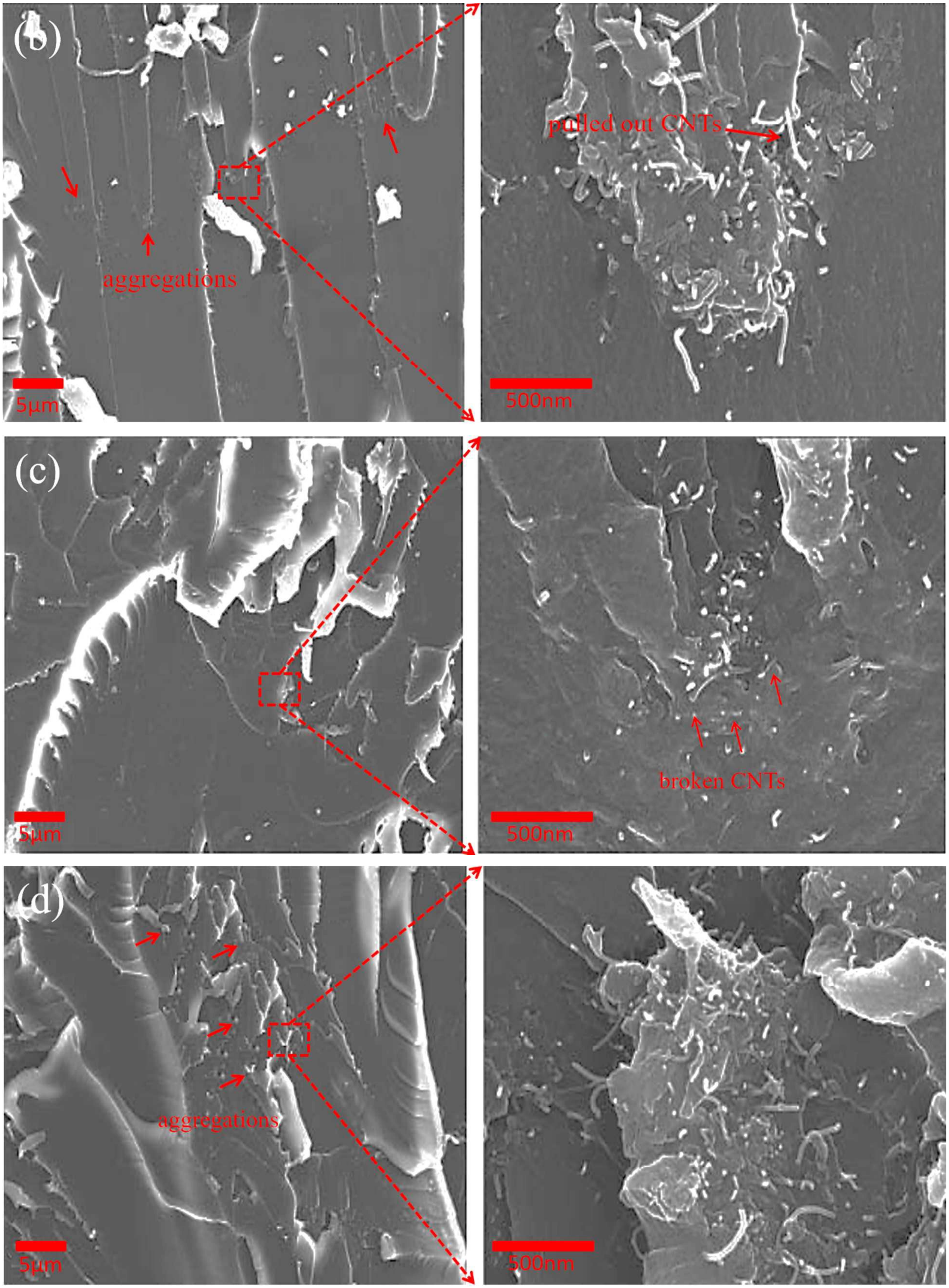
(b)
aggregations
5μm
pulled out CNTs
500nm
(c)
5μm
broken CNTs
500nm
(d)
aggregations
5μm
500nm

Fig. 5. SEM images of pure epoxy (a) and epoxy nanocomposites containing 0.2% p-CNT (b), 0.2% CNT-NH_2 (c), and 0.5% CNT-NH_2 (d) and their magnified images (boxed region).

3.5. Thermal Stability assessment

The effect of CNT on thermal stability of epoxy matrix were evaluated by TGA analysis. The TGA thermograms were analysed by defining two parameters i.e. temperature corresponding to 5% weight loss (T_i) and temperature corresponding to the maximum of TGA derivative (T_{max}) and results are shown in Table 2. As it can be seen, T_i and T_{max} of the epoxy systems are continuously improved with increasing the CNT loading and this improvement in CNT-NH_2/epoxy systems is higher than that of the p-CNT/epoxy systems. However, increase of T_i and T_{max} in nanocomposites having 0.1% CNT loading is negligible in comparison to the pure epoxy and these thermal stability characteristics at 0.2% and 0.5% CNT loadings are more highlighted. At 0.2 % CNT loading, the T_i and T_{max} of CNT-NH_2/epoxy nanocomposites are increased by about 9 ^oC and 7 ^oC, respectively, in comparison to those of p-CNT/epoxy nanocomposites. This clearly indicates that incorporation of amino-functionalized CNT into epoxy matrix lead to an increasing effect on thermal stability compared to the epoxy systems incorporated with p-CNT. The proper interactions between epoxy and CNT-NH_2 can hinder the diffusion of molecules from the matrix under high temperature and thus yields the improved thermal stability of epoxy nanocomposite. However, the epoxy systems containing 0.5% CNT-NH_2 have no significant enhancement in the thermal stability compared to the same p-CNT loading. The T_i and T_{max} values of CNT-NH_2/epoxy nanocomposites having 0.5% loading are increased by only 2^{o}C and 3^{o}C, respectively. This may be attributed to the possible aggregation of CNT at higher loadings.

Table 2. The results of TGA analyses for various epoxy nanocomposites.

	T_i (^{o}C)		T_{max} (^{o}C)	
CNT%	*p-CNT*	*CNT-NH_2*	*p-CNT*	*CNT-NH_2*
0	218.3	218.3	242.6	242.6
0.1	219.8	220.3	243.1	243.8
0.2	225.4	234.7	251.4	258.0
0.5	239.5	241.8	264.7	267.2

4. Conclusions

A straightforward chemistry approach which does not require any harsh acidic oxidation was introduced for preparation of functionalized CNT with primary alkyl amine groups. In a one-step synthesis, 2-aminoethanethiol hydrochloride radicals were clicked onto the CNT surface through its thiol radical head, confirming by appearance of N-H and S-C peaks in FTIR graphs. TGA analysis showed that the amount of functional groups on the surface is lower than those functionalized by oxidative based methods. Epoxy nanocomposites were prepared using various loadings of pure CNT and aminated CNT and then characterized by DMTA, tensile tests, and TGA. Presence of amine groups covalently bonded to CNT improved the interfacial interactions, reflecting in improved thermal and mechanical properties of the epoxy nanocomposites. The DMTA results of epoxy nanocomposites containing 0.2% CNT-NH_2 showed an increase of 10^oC in T_g, compared to the pure epoxy. However, a decrease in T_g was found due to a decreased degree of crosslinking in the nanocomposites containing high CNT-NH_2 loading i.e. 0.5%. Addition of only 0.2 % amino-functionalized CNT improved the tensile strength of nanocomposites by 6.52% and 16.6%, respectively. This enhancement in tensile properties is attributed to the homogenous dispersion and strong interfacial bonding between CNT-NH_2 and the epoxy matrix, which was further confirmed by the SEM observations on fracture surfaces of epoxy nanocomposites. The tensile strength decreased when the CNT loading increased up to 0.5% due to the agglomeration of CNTs and the increased viscosity of the epoxy matrix at the higher CNT loadings. However, the tensile modulus was found to increase even at 0.5% CNT loading, which is due to the enhanced stiffness of the nanocomposites imparted by the reinforcement effect of CNT.

References

1. Iijima S. Helical microtubules of graphitic carbon. nature. 1991;354(6348):56-8.
2. Gojny FH, Wichmann MHG, Fiedler B, Kinloch IA, Bauhofer W, Windle AH, et al. Evaluation and identification of electrical and thermal conduction mechanisms in carbon nanotube/epoxy composites. Polymer. 2006;47(6):2036-45.
3. Yuen S-M, Ma C-CM, Wu H-H, Kuan H-C, Chen W-J, Liao S-H, et al. Preparation and thermal, electrical, and morphological properties of multiwalled carbon nanotubeand epoxy composites. Journal of Applied Polymer Science. 2007;103(2):1272-8.
4. Andrews R, Weisenberger MC. Carbon nanotube polymer composites. Current Opinion in Solid State and Materials Science. 2004;8(1):31-7.
5. Liang W, Yokojima S, Zhou D, Chen G. Localized-Density-Matrix Method and Its Application to Carbon Nanotubes. The Journal of Physical Chemistry A. 2000;104(11):2445-53.
6. Naebe M, Wang J, Xue Y, Wang X, Lin T. Carbon nanotube reinforced rigid-rod polyimide. Journal of Applied Polymer Science. 2010;118(1):359-65.
7. Kuan H-C, Ma C-CM, Chang W-P, Yuen S-M, Wu H-H, Lee T-M. Synthesis, thermal, mechanical and rheological properties of multiwall carbon nanotube/waterborne polyurethane nanocomposite. Composites Science and Technology. 2005;65(11–12):1703-10.

8. Zhou Y, Wu P, Cheng Z, Ingram J, Jeelani S. Improvement in electrical, thermal and mechanical properties of epoxy by filling carbon nanotube. Express polymer letters. 2008;2(1):40-8.

9. Ahmadi M, Masoomi M, Safi S. Mechanical property characterization of carbon nanofiber/epoxy nanocomposites reinforced by GMA-grafted UHMWPE fibers. Composites Part B: Engineering. 2015;83:43-9.

10. Pandey P, Mohanty S, Nayak SK. Improved mechanical and crystallization characteristics of polymer nanocomposites reinforced with carbon nanotube oxidized via wet mechanochemical method. High Performance Polymers. 2014;26(7):760-9.

11. Gojny FH, Schulte K. Functionalisation effect on the thermo-mechanical behaviour of multi-wall carbon nanotube/epoxy-composites. Composites Science and Technology. 2004;64(15):2303-8.

12. Gojny FH, Wichmann MHG, Köpke U, Fiedler B, Schulte K. Carbon nanotube-reinforced epoxy-composites: enhanced stiffness and fracture toughness at low nanotube content. Composites Science and Technology. 2004;64(15):2363-71.

13. Liu L, Wagner HD. Rubbery and glassy epoxy resins reinforced with carbon nanotubes. Composites Science and Technology. 2005;65(11–12):1861-8.

14. Fidelus JD, Wiesel E, Gojny FH, Schulte K, Wagner HD. Thermo-mechanical properties of randomly oriented carbon/epoxy nanocomposites. Composites Part A: Applied Science and Manufacturing. 2005;36(11):1555-61.

15. Khare R, Bose S. Carbon nanotube based composites-a review. Journal of Minerals & Materials Characterization & Engineering. 2005;4(1):31-46.

16. Zhou Y, Pervin F, Lewis L, Jeelani S. Experimental study on the thermal and mechanical properties of multi-walled carbon nanotube-reinforced epoxy. Materials Science and Engineering: A. 2007;452–453:657-64.

17. Im JS, Jeong E, In SJ, Lee Y-S. The impact of fluorinated MWCNT additives on the enhanced dynamic mechanical properties of e-beam-cured epoxy. Composites Science and Technology. 2010;70(5):763-8.

18. Goh PS, Ismail AF, Ng BC. Directional alignment of carbon nanotubes in polymer matrices: Contemporary approaches and future advances. Composites Part A: Applied Science and Manufacturing. 2014;56:103-26.

19. Zabihi O, Khayyam H, Fox BL, Naebe M. Enhanced thermal stability and lifetime of epoxy nanocomposites using covalently functionalized clay: experimental and modelling. New Journal of Chemistry. 2015;39(3):2269-78.

20. Wang J, Yan S, Xie B, Bao R, He Y. Dynamic analysis and mechanical behavior of thermally conductive adhesive reinforced with amine-grafted multiwalled carbon nanotubes. Polymer Composites. 2014;35(5):964-8.

21. Xie X-L, Mai Y-W, Zhou X-P. Dispersion and alignment of carbon nanotubes in polymer matrix: A review. Materials Science and Engineering: R: Reports. 2005;49(4):89-112.

22. Yang K, Gu M, Guo Y, Pan X, Mu G. Effects of carbon nanotube functionalization on the mechanical and thermal properties of epoxy composites. Carbon. 2009;47(7):1723-37.

23. Gojny FH, Wichmann MHG, Fiedler B, Schulte K. Influence of different carbon nanotubes on the mechanical properties of epoxy matrix composites – A comparative study. Composites Science and Technology. 2005;65(15–16):2300-13.

24. Li Q, Church J, Kafi A, Naebe M, Fox B. An improved understanding of the dispersion of multi-walled carbon nanotubes in non-aqueous solvents. J Nanopart Res. 2014;16(7):1-12.

25. Sulong AB, Ramli MI, Hau SL, Sahari J, Muhamad N, Suherman H. Rheological and mechanical properties of carbon nanotube/Graphite/SS316L/polypropylene nanocomposite for a conductive polymer composite. Composites Part B: Engineering. 2013;50:54-61.

26. Yanhong H, Olga AS, Zushou H, Clifford WP, Donald WB. Carbon nanostructures for advanced composites. Reports on Progress in Physics. 2006;69(6):1847.

27. Karousis N, Tagmatarchis N, Tasis D. Current Progress on the Chemical Modification of Carbon Nanotubes. Chemical Reviews. 2010;110(9):5366-97.

28. Syrgiannis Z, Bonasera A, Tenori E, La Parola V, Hadad C, Gruttadauria M, et al. Chemical modification of carbon nanomaterials (SWCNTs, DWCNTs, MWCNTs and SWCNHs) with diphenyl dichalcogenides. Nanoscale. 2015;7(14):6007-13.

29. Ma P-C, Siddiqui NA, Marom G, Kim J-K. Dispersion and functionalization of carbon nanotubes for polymer-based nanocomposites: A review. Composites Part A: Applied Science and Manufacturing. 2010;41(10):1345-67.

30. Eitan A, Jiang K, Dukes D, Andrews R, Schadler LS. Surface Modification of Multiwalled Carbon Nanotubes: Toward the Tailoring of the Interface in Polymer Composites. Chemistry of Materials. 2003;15(16):3198-201.

31. Trojanowicz M. Analytical applications of carbon nanotubes: a review. TrAC Trends in Analytical Chemistry. 2006;25(5):480-9.

32. Kim JA, Seong DG, Kang TJ, Youn JR. Effects of surface modification on rheological and mechanical properties of CNT/epoxy composites. Carbon. 2006;44(10):1898-905.

33. Singh P, Campidelli S, Giordani S, Bonifazi D, Bianco A, Prato M. Organic functionalisation and characterisation of single-walled carbon nanotubes. Chemical Society Reviews. 2009;38(8):2214-30.

34. Van Thu L, Cao Long N, Quoc Trung L, Trinh Tung N, Duc Nghia N, Minh Thanh V. Surface modification and functionalization of carbon nanotube with some organic compounds. Advances in Natural Sciences: Nanoscience and Nanotechnology. 2013;4(3):035017.

35. Verma ML, Naebe M, Barrow CJ, Puri M. Enzyme Immobilisation on Amino-Functionalised Multi-Walled Carbon Nanotubes: Structural and Biocatalytic Characterisation. PLoS ONE. 2013;8(9):e73642.

36. Jaffe RL. Quantum Chemistry Study of Fullerene and Carbon Nanotube Fluorination. The Journal of Physical Chemistry B. 2003;107(38):10378-88.

37. Gojny FH, Nastalczyk J, Roslaniec Z, Schulte K. Surface modified multi-walled carbon nanotubes in CNT/epoxy-composites. Chemical Physics Letters. 2003;370(5–6):820-4.

38. Yan Y, Cui J, Zhao S, Zhang J, Liu J, Cheng J. Interface molecular engineering of single-walled carbon nanotube/epoxy composites. Journal of Materials Chemistry. 2012;22(5):1928-36.

39. Mittal V. Optimization of polymer nanocomposite properties: John Wiley & Sons; 2009.

40. Kim MT, Rhee KY, Park SJ, Hui D. Effects of silane-modified carbon nanotubes on flexural and fracture behaviors of carbon nanotube-modified epoxy/basalt composites. Composites Part B: Engineering. 2012;43(5):2298-302.

41. Ma P-C, Mo S-Y, Tang B-Z, Kim J-K. Dispersion, interfacial interaction and re-agglomeration of functionalized carbon nanotubes in epoxy composites. Carbon. 2010;48(6):1824-34.

42. Mittal V. Surface modification of nanotube fillers: John Wiley & Sons; 2011.

43. Avilés F, Sierra-Chi CA, Nistal A, May-Pat A, Rubio F, Rubio J. Influence of silane concentration on the silanization of multiwall carbon nanotubes. Carbon. 2013;57:520-9.

44. González-Domínguez JM, González M, Ansón-Casaos A, Díez-Pascual AM, Gómez MA, Martínez MT. Effect of Various Aminated Single-Walled Carbon Nanotubes on the Epoxy Cross-Linking Reactions. The Journal of Physical Chemistry C. 2011;115(15):7238-48.

45. Ma PC, Kim J-K, Tang BZ. Effects of silane functionalization on the properties of carbon nanotube/epoxy nanocomposites. Composites Science and Technology. 2007;67(14):2965-72.

46. Kathi J, Rhee K-Y, Lee JH. Effect of chemical functionalization of multi-walled carbon nanotubes with 3-aminopropyltriethoxysilane on mechanical and morphological properties of epoxy nanocomposites. Composites Part A: Applied Science and Manufacturing. 2009;40(6–7):800-9.

47. Cui L-J, Wang Y-B, Xiu W-J, Wang W-Y, Xu L-H, Xu X-B, et al. Effect of functionalization of multi-walled carbon nanotube on the curing behavior and mechanical property of multi-walled carbon nanotube/epoxy composites. Materials & Design. 2013;49:279-84.

48. Shen J, Huang W, Wu L, Hu Y, Ye M. The reinforcement role of different amino-functionalized multi-walled carbon nanotubes in epoxy nanocomposites. Composites Science and Technology. 2007;67(15–16):3041-50.

49. Coleman KS, Bailey SR, Fogden S, Green MLH. Functionalization of Single-Walled Carbon Nanotubes via the Bingel Reaction. Journal of the American Chemical Society. 2003;125(29):8722-3.

50. Temel G, Uygun M, Arsu N. Modification of multiwall carbon nanotube by thiol-ene click chemistry. Polym Bull. 2013;70(12):3563-74.

51. Luong ND, Sinh LH, Johansson L-S, Campell J, Seppälä J. Functional Graphene by Thiol-ene Click Chemistry. Chemistry – A European Journal. 2015;21(8):3183-6.

52. Lowe AB. Thiol-ene "click" reactions and recent applications in polymer and materials synthesis. Polymer Chemistry. 2010;1(1):17-36.

53. Nilsson C, Simpson N, Malkoch M, Johansson M, Malmström E. Synthesis and thiol–ene photopolymerization of allyl-ether functionalized dendrimers. Journal of Polymer Science Part A: Polymer Chemistry. 2008;46(4):1339-48.

54. Hoyle CE, Bowman CN. Thiol–Ene Click Chemistry. Angewandte Chemie International Edition. 2010;49(9):1540-73.

55. Nakka JS, Jansen KMB, Ernst LJ, Jager WF. Effect of the epoxy resin chemistry on the viscoelasticity of its cured product. Journal of Applied Polymer Science. 2008;108(3):1414-20.

56. Zabihi O, Hooshafza A, Moztarzadeh F, Payravand H, Afshar A, Alizadeh R. Isothermal curing behavior and thermo-physical properties of epoxy-based thermoset nanocomposites reinforced with Fe2O3 nanoparticles. Thermochimica Acta. 2012;527:190-8.

57. Li GZ, Wang L, Toghiani H, Daulton TL, Koyama K, Pittman CU. Viscoelastic and Mechanical Properties of Epoxy/Multifunctional Polyhedral Oligomeric Silsesquioxane Nanocomposites and Epoxy/Ladderlike Polyphenylsilsesquioxane Blends. Macromolecules. 2001;34(25):8686-93.

58. Zabihi O, Ghasemlou S. Nano-CuO/Epoxy Composites: Thermal Characterization and Thermo-Oxidative Degradation. International Journal of Polymer Analysis and Characterization. 2012;17(2):108-21.